Parametric Fault Modeling and Diagnostics of a Turbofan Engine

S. Ganguli, *Student Member, IEEE,* S. Deo, and D. Gorinevsky, *Senior Member, IEEE*

***Abstract* — A parametric fault modeling and diagnostics approach of a turbofan engine is presented. The healthy engine model is obtained as a steady state map between input parameters representing engine operating conditions and output parameters governing engine performance characteristics. The fault modeling is conceptualized as either degraded engine performance levels or as sensor failures and both incipient and abrupt fault scenarios are considered. The fault parameters are successfully estimated using Generalized Least Squares (GLS) techniques with data obtained from several recorded flight data. Further, a nonlinear estimation method is introduced to improve the diagnostic performance in certain cases of large and abrupt failures.**

I. Introduction

Research in the area of engine fault diagnostics concentrates on finding automatic diagnosis tools and improving diagnostics reliability. The traditional approach of automated diagnostics involves establishing a library of faults, based on field experience, manufacturer data or test/flight data, and building an expert system to identify potential source of failure. However, the reliability of such methods depends greatly on the accuracy of the faults identified during inspection and on the size of the knowledge basis. The state of the art research in engine fault diagnostics has effectively advanced in two major directions. One approach combines traditional rule-based diagnostics method (e.g., expert systems) with other AI techniques, such as neural networks and fuzzy logic [1], [2]. The other approach uses models of engine performance and is known as model-based fault diagnostics [3], [4]. Model-based diagnostics mainly consists of combining theoretical knowledge with test/flight data. Here, an estimated system model is compared to a nominal system model. The residual or error between the two models provides a measure of the deviation between the estimated and nominal models, and is used to make a decision as to whether a failure has occurred or not. An essential requirement for model-based diagnostics is the development of an accurate system model. Reference [5] provides an excellent survey of engine health monitoring systems for commercial aircrafts.

This paper presents parametric fault modeling and diagnostics of the LF507 turbofan engine manufactured by Honeywell. LF507 is a two-spool aircraft engine used at regional jet aircrafts, such as BAE Avro RJ85. The typical faults affecting the LF507 engines and considered in this research include deterioration of the turbine efficiency, combustor liner failure, leakage in the engine bleed system and sensor failures in the exhaust gas temperature. The fault modeling is based on minimizing the least squares error between recorded flight data and a simulated engine model. Sensor data related to engine performance characteristics along with flight condition sensor measurements were collected at each flight cycle. These are typically sampled once or twice per flight, logged and transferred to a ground monitoring system and were available for the off-line engine model development. This research was performed as a part of the PTM (Predictive Trend Monitoring) system development sponsored by Honeywell Engine Systems and Services. The engine fault model aims at facilitating predictive maintenance of Honeywell aircraft engines. However, the research presented in this paper also has greater applicability – to model-based estimation for trending of a broad range of aerospace systems.

II. Basic theory for fault estimation

The theoretical background of engine fault modeling and diagnostics is presented in this section. The engine fault simulation model is shown schematically in Fig. 1. In this setup, the vectors of *operating condition* data and *output* data are known at each flight cycle. The engine fault modeling involves determining the *fault parameter* vector. In effect, this estimation problem requires inverting the model map in Fig. 1 with respect to the *fault parameter* vector input. The problem is compounded by the fact that the data used for the estimation is distorted by sensor noise and that modeling error is present.

The basic approach to fault diagnostics is to remove the map dependency on the *operating condition* vector input and then to evaluate the *fault parameter* vector through an optimal statistical estimation algorithm. The functional dependency of the *output* vector is linearized w.r.t. the *fault parameter* vector, which leads to a least squares-type estimation problem. The fault model obtained using the linear assumption is further validated against the nonlinear functional relationship between the *output* vector and the *fault parameters*. The technical details are discussed in the following paragraphs.

The engine model in Fig. 1 can be presented in the form

$$\hat{y} = f(x, p), \tag{1}$$

where $\hat{y} \in \mathbf{R}^m$ is the model-based prediction of the vector y, $x \in \mathbf{R}^n$ is the vector of measured operating conditions, and $p \in \mathbf{R}^l$ is the vector of performance deterioration parameters/sensor error parameters in the model. The function $f(\cdot,\cdot)$ in the model might be unavailable in an analytical form, but can be computable point-wise by

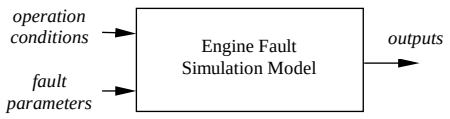

Fig. 1. Schematic diagram of engine fault simulation model.

running a simulation. In the no-fault or nominal case, where no deterioration/failure has occurred, it is assumed that $p = 0$. The residual, *r*, is computed as the difference between actual engine output data *y*, and estimated output $\hat{y}$, by assuming that no performance deterioration/failure has occurred, i.e., $p = 0$ in (1). In other words, the residual is given by

$$r = y - f(x,0). \quad (2)$$

Thus, for an accurate model and no failure/deterioration, we expect to get $r = 0$. A failure or degraded performance can be modeled by the fault parameter vector *p*. This vector can be estimated from the residual *r* by inverting the map $f(x,\cdot)$. One apparent difficulty in this approach is the nonlinearity of the function $f(\cdot,\cdot)$. Fortunately, in many practical applications this difficulty can be overcome by linearizing (1) around the nominal model where $p = 0$. In case of incipient faults like performance deterioration, the magnitude of the fault parameters (fault intensity) is usually small. For instance, a turbine efficiency drop of just 1% might be considered serious enough to pull off the turbomachine. Thus, a sufficiently accurate approximation of the model in (1) is given by

$$\hat{y} = f(x,0) + Sp, S = \left.\frac{\partial f(x,p)}{\partial p}\right|_{p=0}, \quad (3)$$

where the Jacobian $S \in \mathbf{R}^{m \times l}$ will be hereafter called the fault sensitivity matrix. The sensitivity matrix *S* in (3) can be numerically estimated by a *secant* method: by incrementing the argument *p* and computing corresponding variation in the output vector $\hat{y}$ in (1). The secant estimate for a column $S^{(j)}$ of the sensitivity matrix *S* is given by

$$S^{(j)} \approx \left[\frac{f(x, se^{(j)} - f(x,0)}{s}\right], \quad (4)$$

where *s* is the secant step size and $e^{(j)}$ is the unit vector directed along the coordinate axis *j*. The parameter *s* should be chosen to provide an optimal tradeoff between the numerical accuracy (limited if *s* is too small) and the nonlinearity error (larger for larger *s*). Linearization of nonlinear maps and use of sensitivities to various efficiency deterioration parameters is well known and commonly practiced in performance analysis of turbomachines.

Combining (2) and (3) yields the residual as

$$r = Sp + e_o, \quad (5)$$

where e_o is the 'noise' term added to reflect *output modeling error* and influence of various factors not accounted for by the model in (3). Thus, the fault modeling and diagnostics effectively involves obtaining an estimate of the fault intensity *p*. We use statistically optimal estimation, such as the Maximum A posteriori Estimate (MAE) or the Maximum Likelihood Estimate (MLE). The basis for such approach is an assumption that the 'noise' e_o in (5) is a normally distributed random variable with zero mean and covariance Q_o: $e_o \sim N(0, Q_o)$. The numerical value of the covariance matrix Q_o can be empirically estimated from the residuals of a population of engines in the absence of faults. Assume further that *p* in (5) is a normally distributed random variable with a zero mean and covariance R as $p \sim N(0, R)$. The covariance matrix *R* reflects prior knowledge of intensity of fault variation encountered in the estimation problem. This covariance will be further considered as a tuning knob parameter of the estimation algorithm devoid of a physical meaning.

Now consider finding a Maximum A posteriori Estimate (MAE) for *p*. With the residual *r* known, the Bayes-rule yields the logarithmic distribution of the conditional probability for the fault *p* as

$$-\log P(p \mid r) = -\log P(r \mid p) - \log P(p) + c, \quad (6)$$

where $c = \log P(r)$ does not depend on *p*, and $P(p)$ is given by $N(0,R)$. Note that in accordance with (5) and distribution of e_o, the conditional probability distribution $P(r \mid p)$ is given by $N(Sp, Q_o)$. By plugging these Gaussian distributions into (6) and minimizing the result we obtain the optimal estimate of *p* as

$$\hat{p} = \arg\min\left[-\log P(p \mid r)\right]$$

$$= \arg\min\left[\frac{1}{2}(r - Sp)^T Q_o^{-1}(r - Sp) + \frac{1}{2} p^T Q_o^{-1} p + \text{const}\right].$$

By differentiating the R.H.S. of (7) with respect to *p* and equating the result to zero, the optimal estimate $\hat{p}$ is found to be

$$\hat{p} = \left[R^{-1} + S^T Q_o^{-1} S\right]^{-1} S^T Q_o^{-1} r. \quad (8)$$

This is also know as the Generalized Least Squares (GLS) estimate of *p*. Assuming no *a priori* information about *p* is available is equivalent to assuming a very large covariance *R* in the distribution for (8) and leads to a Maximum Likelihood Estimate (MLE). The MLE is obtained from the MAE by substituting a zero for R^{-1} and has the form

$$\hat{p} = \left[S^T Q_o^{-1} S\right]^{-1} S^T Q_o^{-1} r. \quad (9)$$

Equation (9) serves as the basis for developing the engine fault model and related diagnostics.

III. Engine Fault Model Development

This section presents a *fault model* of the engine that is used for fault diagnostic system development, verification and validation. The fault modeling involves addition of engine failure modes in a modular fashion to the healthy or the no-fault engine model.

The healthy engine is modeled as a sequence of interconnected components [6]. Ambient air is sucked into the engine by the inlet fan and is split at the plenum; a part enters the compressor section while the rest is bypassed. The flow of the air is guided by inlet guide vanes. High pressure air from the compressors enters the combustor where fuel is injected through annular nozzles. Hot gases from the combustor expand in the gas turbine section, which drives the fan and the engine shafts (concentrically arranged). Exhaust gases from the turbine along with the bypassed air is expelled outside the aircraft via the nozzle and the kinetic energy of the exhaust is available as the engine thrust. The bleed band section is used by the engine control system to maintain efficient engine operations during transient stages, e.g., starting periods of engine acceleration. Conditions of steady-state engine operation are measured by four parameters: altitude (*h*), Mach No (*Mach*), total air temperature (*TAT*), engine fan speed (*N1*),

and the engine performance characteristics is measured by three outputs: engine core speed (*N2*), exhaust gas temperature (*EGT*), fuel flow (*WF*).

Many of the incipient and abrupt faults that result in the deterioration of engine performance can be modeled as adverse changes in the parameters that affect the turbine efficiency and bleed band efficiency. The fault modeling involves lumping parameters like efficiencies to capture performance deterioration. Consequently, detection of these faults can be performed by identifying deviations of performance parameters from their nominal values. In addition, typical sensor failures are also considered in the engine fault model – specifically for exhaust gas temperature (*EGT*) measurements. These are modeled by introducing an additive error term in the *EGT* measurement. These fault parameters considered are:

1. p_1 – performance loss for the high pressure turbine;
2. p_2 – leakage in the bleed band system;
3. p_3 – *EGT* sensor measurement error.

These faults make a fault parameter vector $p = [p_1 \quad p_2 \quad p_3]^T$. The intensities of these fault parameters were estimated based on recorded flight data for differnet engines and flights. The fault parameter vector can effectively capture the following six categories of faults:

1. HP Turbine Performance Degradation
2. Combustor Liner Failure
3. Bleed Band Leakage
4. Bleed System Failure
5. EGT Sensor Drift
6. EGT Sensor Failure

Both high pressure performance degradation and combustor liner failure cause an increase in the residual of *N2*, and a decrease in *EGT* and *WF*. This effect is well captured by a corresponding change in the high pressure turbine efficiency. Faults in the bleed band section cause an increase in all the three residuals ($\Delta N2$, ΔEGT, ΔWF) and are effectively modeled by a bleed band efficiency factor. Faulty *EGT* sensor measurements are taken into account by a corresponding additive fault parameter.

The faults 1,3,5 develop gradually, their intensities grow incrementally with time. The faults 2,4, and 6 occur abruptly, they become fully developed at some flight, while little or no fault effect was observed in the previous flight data.

This study used snapshot data collected from engine during aircraft takeoff, when it runs at maximum power. This data is routinely collected in the operation and was available for our study. Typically each flight (and hence each engine) was operated 3-4 times a day. One data-point consists of snapshot measurements of engine input and output parameters per flight.

The details of engine fault modeling are presented next.

A. No-fault Model Bias Error and Noise

For determining bias error and noise (scatter) of the model prediction, data from six different engines was used. Each dataset contained about 150-450 data-points. The residuals ($\Delta N2$, ΔEGT, ΔWF) are calculated for the fault-free engine model to estimate modeling errors not accounted for in the engine model. A bias error was observed in the residuals (approximately constant for individual engines). This is modeled by a normally distributed random variable as $bias \sim N(\mu_{bias}, Q_{bias})$. The numerical values of μ_{bias} and Q_{bias} were computed based on the first 50 points of each dataset. This is done (not using entire datasets) to avoid an accidental capture of minor degradation in engine performance over time – a natural phenomena for all engines. The bias error is implemented in the engine fault model by seeding a corresponding random number and adding the error terms to the engine outputs: *N2*, *EGT* and *WF*. Note that for the residual calculations in the fault scenarios, the same technique (averaging over first 50 points) is used to remove bias errors.

The output noise covariance matrix, $Q_{o,}$ is calculated based on the nominal datasets by computing the output covariance matrix for each engine and taking an average across the datasets. Together, the two normally distributed random variables e_o and *bias* define the sensor noise/modeling error at the output of the engine model.

B. HP Turbine Performance Degradation (HPG)

The fault parameter representing HPG fault is estimated based on datasets from four engines. The effect of HP turbine efficiency degradation results in a gradual decrease in the residual $\Delta N2$ and gradual increases in the residuals ΔEGT and ΔWF. Each dataset contains 1000-2000 data-points and the fault is spread over approximately 1000 data-points. The fault is effectively captured by a linear function of the parameter p_1. Least squares data-fitting techniques are used to determine this function for each dataset and then averaged over the four engines. The slopes of the changes in p_1 for the different engines were calculated as:

1. Engine M91: 2.0671 % /1000 data-point
2. Engine M88: 1.1810 % /1000 data-point
3. Engine M72: 0.5682 % /1000 data-point
4. Engine M89: 0.7420 % /1000 data-point

Thus, for fault-type HPG, the fault parameter p_1 can be modeled as a normally distributed random number with mean and variance computed as:

$$p_{1,HPG} \sim N(1.1396, 0.4488). \quad (10)$$

C. Combustor Liner Failures (HPA)

Two sets of data were available to estimate the combustor liner failure. These data sets were extracted from historical data and correspond to the actual operational cases of the failure. The exact type of the failure was confirmed by the repair and overhaul analysis. Fig. 2 shows the plots for Engine M83. The effect of combustor liner failure is an abrupt decrease in the residual $\Delta N2$ and abrupt increases in the residuals ΔEGT and ΔWF. This pattern of change in the residuals is modeled by a respective change in the fault parameter p_1. The last 9 few data-points (shown by '+' signs in Fig. 2) represent this fault and correspond to a change in p_1 by 1% or more. Statistically, this phenomenon can be represented by a normally distributed random number with the mean and variance given by:

$$p_{1,HPA} \sim N(1.4975, 0.0743). \quad (11)$$

D. Bleed Band Leakage (BBG)

Only one set of data was available for modeling failures categorized as bleed band leakages: Engine M94. A leakage in the bleed band section of the engine causes an increasing

pattern in all the three residuals $\Delta N2$, ΔEGT and ΔWF. The corresponding change in the bleed band efficiency (fault parameter p_2) is estimated as a linear variation with time by minimizing the least-squares error. The slope of the change in p_2 is 0.39% per data-point for this particular dataset. A statistical representation of the corresponding fault parameter $p_{2,BBG}$ awaits further collection of data corresponding to BBG-type faults.

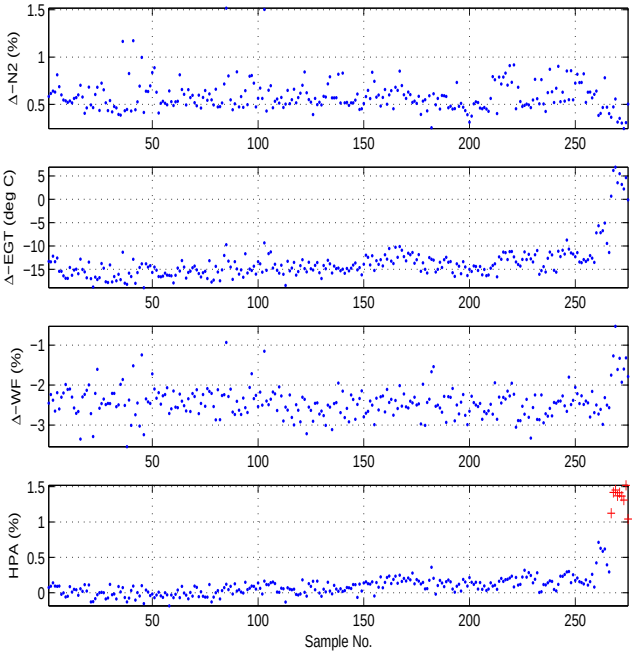

Fig 2. M83:HPA fault data. Residuals and fault parameter are shown.

E. Bleed Band Failure (BBA)

The bleed band abrupt failure model is developed based on seven sets of data. The residuals are generated by comparing the actual engine input-output measurements with the estimated healthy engine outputs. For all cases, the estimated leakages are of the order of 20% to 25% A normally distributed random number with the following mean and variance can be use to predict this type of failure:

$$p_{1,BBA} \sim N(21.457, 73.815)\,. \qquad (12)$$

The high variance of $p_{1,BBA}$ is due to the two atypical data-points (3% and 5%). Also, observe that the mean value of the estimated fault parameter is considerably high as compared to the secant-step size of 1% used for estimation. The secant-step size was chosen sufficiently small to approximate the engine input-output map with a linear function. Since, it is not possible to know *a priori* the size of the fault using the secant-method, the model needs to be validated whenever the estimated fault intensity gets extrapolated outside its assumed linear region.

F. EGT Sensor Failure (EGA)

Only one dataset was available to develop a fault module representing abrupt EGT sensor failure. All the residuals showed an initial drift. This is due to an efficiency loss in the HP turbine section causing an extra offset of approximately 10 deg C before the EGT sensor failure occurs. The last portion of the data shows an abrupt jump in the EGT residual. The mean and variance of the data-points after failure are computed as 42 deg C (removing 10 deg initial offset) and 18 deg C respectively. However, this is the statistical estimate based upon one failure case.

Note that the EGT sensor measurement is an average of an array of several thermocouples and can fail in a multiple number of ways. The exact array structures and failure modes were not available for modeling. However, based upon several discussions with field experts it was noted that EGT sensor failures typically varied between –15 to –60 deg C and +15 to +60 deg C (without recorded data to confirm). Based on this knowledge, one can model this failure by a random number ($p_{3,EGA}$) varying between the specified ranges.

IV. Engine Fault Model Validation

The LF507 engine fault simulation model is developed based on a linear relationship between the fault parameters and the engine outputs. The linear approximation is sufficient when the estimated fault intensities are relatively small and can be successfully used for modeling small gradual faults. However, in case of abrupt failures and faults of higher intensities, the suitability of linear approximation needs to be verified against the actual behavior of the function relating engine outputs with fault parameters. Amongst the three fault parameters p_1, p_2 and p_3, the last parameter, representing *EGT* abrupt and gradual faults, enters the fault model by direct addition to one of the engine outputs (specifically, the *EGT* sensor measurement). This map function between the engine outputs and the fault parameter is perfectly linear and the linear fault estimation is accurate in this case. However, the efficiency parameters p_1 and p_2 enter the detailed engine gas path model in a complicated way. Thus, it needs to be determined how these two fault parameters affect the outputs.

Fig. 3 (a) shows a comparison of the actual input-output function with its linear approximation used for estimation of HP performance degradation. The engine input conditions are selected as a typical takeoff data-point: h = 1000 ft, *Mach* = 0.2, *TAT* = 10 deg C and *N1* = 90%. Since both $p_{1,HPG}$ and $p_{1,HPA}$ are estimated to be in the range of 1% to 2%, the HP turbine efficiency was deteriorated up to a maximum of 4%. The linear model outputs are generated by interpolating/extrapolating the engine outputs at 1% fault over the entire range (secant step-size was chosen as 1%). It is observed that the linear approximation matches well the nonlinear input-output function for the estimated fault intensity range. Fig. 3 (b) shows a similar comparison for estimation of bleed band leakage faults with the same engine input conditions as before. Unlike HPG/HPA faults, the ranges for BBG and BBA faults differ. For gradual bleed band faults, the fault parameter in the range of up to 12%. However, the abrupt failures are estimated to lie in a range of up to 25%. The linear model outputs are generated by interpolating/extrapolating the engine outputs at 1% fault over the entire range, as secant step-size was selected as 1% for estimation (secant step-size was chosen as 1%). From Fig. 3 (b) it is observed that the linear model deviates from the actual nonlinear function considerably for efficiencies over 15%. However, the fault model developed based on the linear approximation is considered adequate for the following reason. From diagnostics viewpoint, it is usually a

challenge to identify gradual faults (unlike abrupt faults). A diagnostic algorithm capable of identifying incipient faults is typically successful in cases of large abrupt failures.

V. Linear and Nonlinear Fault Estimation

This section presents estimation of engine faults based on the model developed in the preceding sections.

Initially a linear model was used, as described in Section II, by making a linear approximation of the engine input-output map. A known covariance of the fault intensities (R) is used for the purpose of estimation. Based on the general order of the fault intensities (1% for HPG/HPA, 5% BBG/BBA, 30 deg C for EGG/EGA) R was chosen as diag{1, 25, 900}. Fig. 4 shows the plots of fault estimates for a typical fault case data. The data were obtained from the flight computer during takeoff. The case was earlier classified as having HPG fault. The idea is to see whether the fault estimates show these failure signatures successfully. It is observed that the bleed-band leakage increases from sample 100 to 121 while the HP turbine deterioration and EGT sensor offset estimates remain small. Thus, we observe satisfactory decoupling in the estimated fault modes. Linearity approximation may be sufficient for diagnosis and identification of the incipient fault mode, but may lead to inaccurate estimation of the fault intensity as the fault develops. A modification of the linear fault estimation approach of Section II was developed to accommodate for the nonlinearity in the function relating outputs to fault parameters.

Consider the residual model of Section II. Introduce a nonlinear term $g=g(x,p)$ to capture the nonlinear dependence on the fault parameter in the residual map. Thus (3) is modified to

$$\hat{y} = f(x,0) + Sp + g,\ S = \left.\frac{\partial f(x,p)}{\partial p}\right|_{p=0}. \qquad (13)$$

The function g cannot be derived analytically but is determined by studying the nonlinear behavior of the simulation model. Note that no matter what form $g(x,p)$ takes, $g(x,0)$ and $\frac{\partial g}{\partial x}(x,0)$ are always zero. Unlike S, there is no generic formula for calculating g numerically. Combining (2) and (13) gives us

$$r = Sp + g + e_o. \qquad (14)$$

Following a similar argument as in Section II, it can be shown that the optimal estimate of the fault parameter satisfies the equation

$$\hat{p} = \left[R^{-1} + S^T Q_o^{-1} S\right]^{-1}\left[S^T Q_o^{-1}(r-g) + \frac{\partial g}{\partial p}^T Q_o^{-1}(r - S\hat{p} - g)\right] \qquad (15)$$

Note that (15) is an implicit equation in $\hat{p}$ and in some cases may require iterative equation solver (MATLAB command *fsolve*) to obtain a solution. In this work an approximate quadratic model of the nonlinearity g is used. This model was developed by performing simulations of the prediction model for varying inputs and determining a simple form of the quadratic nonlinearity g that provides a sufficiently accurate approximation of the nonlinear behavior of the model. A detailed numerical study found that a very simple quadratic model suffices. We use a nonlinearity model that is fixed, independent of the ambient conditions and other variables that are included in the vector x. Moreover, it is assumed that $g(x,p)=g(p)$. In a most general case, the quadratic term $g=g(p)$ is

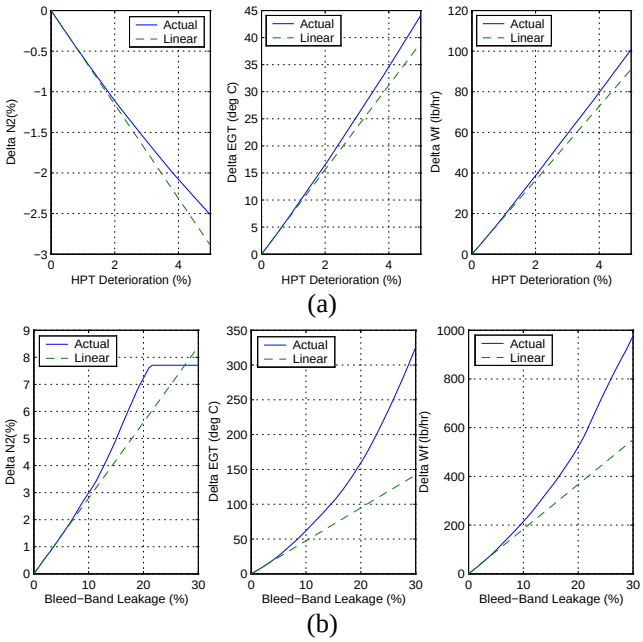

Fig 3. (a) Comparison of the actual input-output function with its linear approximation used for estimation of HP performance degradation; (b) comparison of the actual input-output function with its linear approximation used for estimation of bleed band leakage faults.

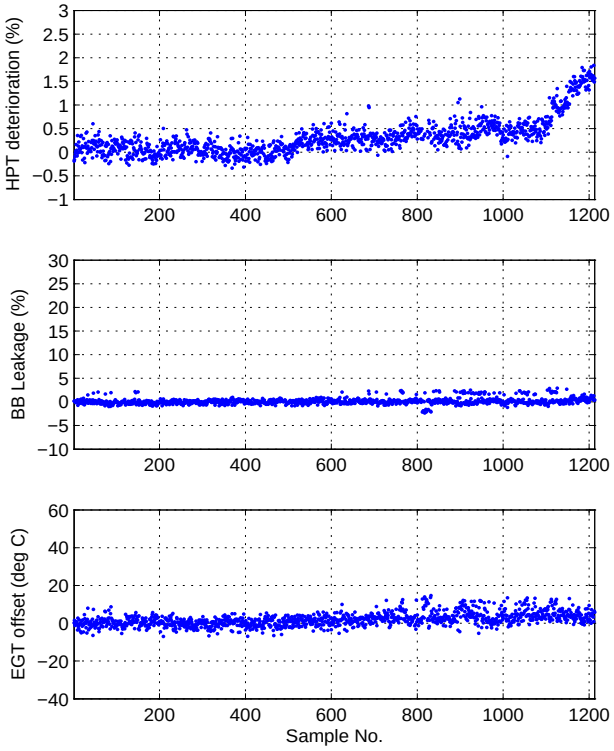

Fig 4. Engine M72: Linear fault estimation of HPG fault data.

characterized by $(m\times l)\times(l+1)/2=18$ coefficients. This is because the quadratic term also has cross terms. Extensive simulations using the engine takeoff model were used to determine which of these terms to retain in the model. It was found that the most important term than needs to be taken into account is the quadratic nonlinearity in the bleed-loss intensity. All other quadratic terms and cross-terms can be conveniently neglected. The function $g(p)$ was therefore chosen to be

$$g(p)=S_2 p^2, \tag{16}$$

where the vector $S_2 \in \mathbf{R}^{3\times 1}$ and is further called the quadratic sensitivity of the bleed band leakage fault. To calculate S_2, we used a best-fit least-squares method. We set HPT deterioration and EGT sensor offset to zero and vary bleed-band leakage in increments in the interested range. We then calculate the residual error and fit a regression model of the form (16) to that data. The numerical value of S_2 was thus determined as

$$S_2=\begin{bmatrix}0.0037 & 0.1529 & 0.3608\end{bmatrix}^T. \tag{17}$$

Using the definition of $g(p)$ from (18), we get

$$\frac{\partial g}{\partial p}=\begin{bmatrix}0 & & 0\\ 0 & 2S_2 p_2 & 0\\ 0 & & 0\end{bmatrix}. \tag{18}$$

Substituting (16) to (18) into (15) gives the optimal estimate of p.

The nonlinear fault estimation algorithm for engine was first validated through simulations. Since the nonlinear correction is meant for cases in which there is large bleed band leakage, a distinct difference between the results of the linear and the nonlinear algorithm is seen only for those cases. Therefore, we chose engines which had experienced a bleed-band leakage fault and compared the results of using the linear and nonlinear estimation algorithms for these engines. The plots in Fig. 5 show the results based on the nonlinear estimation algorithm for an engine which had an abrupt bleed band leakage failure. The corresponding linear estimation algorithm (not shown) led to a spurious rise of approximately 12 deg C in EGT sensor offset in the last data-point. The nonlinear estimation algorithm reduces this inaccurate estimation by half. Also, the nonlinear estimation algorithm reduces the magnitude of the bleed-band leakage from approximately 24% (not shown) to 17%. Not much change is observed in the HP turbine deterioration estimates.

VI. Conclusion

This paper presents a parametric fault modeling and diagnostics approach for a typical turbofan engine. The benefit of parametric fault modeling is that various failure signatures can be effectively captured by a selected number of parameters. However, a key assumption is that certain kinds of engine failures will result in specific changes in the parameters being monitored. The residual modeling was based on minimization of the least squares error between actual and estimated data. Fault parameters were estimated using a linear approximation of the map relating the fault parameters and the residuals. Faults of both abrupt and gradual nature were successfully modeled using this technique. The developed fault model was validated against actual nonlinear engine input-output function. Linear approximation of the engine map used during the modeling stage was found inadequate for one of the fault cases. To further improve the accuracy of the estimation algorithm and minimize cross-coupling of fault estimates, the nonlinear behavior of the engine model is investigated. A simple nonlinear approximation of the model was developed and used in a new optimal nonlinear stochastic estimation algorithm. Implementation of this algorithm shows improvements in the fault estimate accuracy for large bleed faults, the ones that caused inaccuracies with linear estimation.

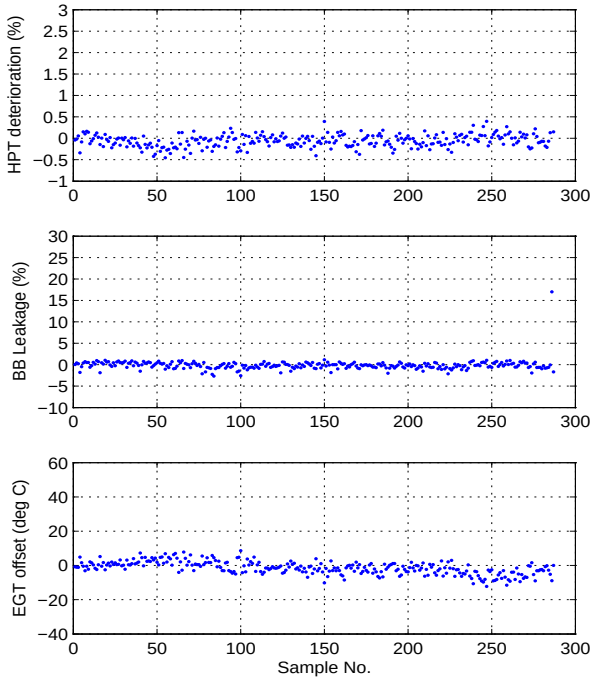

Fig 5. Engine M23: Nonlinear fault estimation of BBA fault data.

Acknowledgment

The authors wish to thank Hanif Vhora, Dale Mukavetz, Charles Ball, Sachi Dash, Dennice Gayme, Dinkar Mylaraswamy and Sunil Menon for their help with various aspects of the engine modeling and data processing.

References

[1] H. R. DePold and F. D. Gass, "The application of expert systems and neural networks to gas turbine prognostics and diagnostics", *ASME Journal of Engineering for Gas Turbines and Power*, vol. 121, no. 4, pp. 607-612, Apr. 1999.

[2] M. M. Polycarpou, "An on-line approximation approach to fault monitoring, diagnosis, and accommodation", *SAE Trans. – Journal of Aerospace*, vol. 103, no. 1, pp. 371-380, 1994.

[3] G. Merrington, "Fault diagnosis in gas turbines using a model-based technique", *ASME Journal of Engineering for Gas Turbines and Power*, vol. 116, pp. 374-380, Apr. 1994.

[4] D. Gorinevsky, E. Nwadiogbu, and D. Mylaraswamy, "Model-based diagnostics for small-scale turbomachines", *41st IEEE CDC*, Las Vegas NV, Dec. 10-13, 2002.

[5] I. Y. Tumer and A. Bajwa, "A suvery of aircraft engine health monitoring systems", *35th AIAA/ASME/SAE/ASEE Joint Propulsion Conf. and Exhibit*, Los Angeles, CA, June 20-24, 1999.

[6] A. Marcos and D. Mylaraswamy, *LF507-F1 Engine General Description and Simulation Model Validation*, Honeywell ES&S, Minneapolis, 2003.